

Surface-Enhanced Infrared Absorption Spectroscopy (SEIRAS) of Light-Activated Photosynthetic Reaction Centers from *Rhodobacter sphaeroides* Reconstituted in a Biomimetic Membrane System

Vedran Nedelkovski,[†] Andreas Schwaighofer,[†] Colin A. Wraight,[‡] Christoph Nowak,^{†,§} and Renate L. C. Naumann^{†,*}

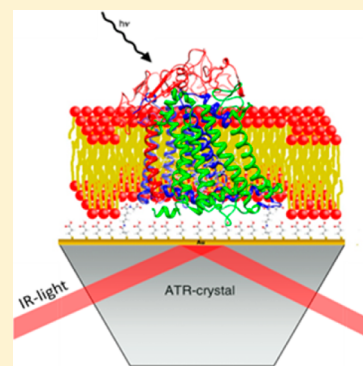
[†]Austrian Institute of Technology GmbH, AIT, Donau-City Str. 1, 1220 Vienna, Austria

[‡]Department of Biochemistry and Center for Biophysics and Computational Biology, University of Illinois, Urbana, Illinois 61801, United States

[§]Center of Electrochemical Surface Technology, CEST, Viktor-Kaplan-Straße 2, 2700 Wiener Neustadt, Austria

Supporting Information

ABSTRACT: Surface-enhanced IR absorption spectroscopy (SEIRAS) in the ATR configuration has been performed on reaction centers (RCs) from *R. sphaeroides*. Surface-enhancement is achieved by a thin, structured gold film present on the surface of an ATR crystal. Purified RCs are immobilized as a monolayer on top of the gold film via a poly histag engineered to the C-terminal end of the M subunit. Subsequently, the RCs are reconstituted into a lipid bilayer by in situ dialysis. Light-minus-dark absorbance spectra were recorded under continuous illumination using the spectrum in the dark as the reference. A number of strong bands have been observed indicating the excitation of the special pair as well as alterations of quinone/quinol species. Spectra were recorded at different time intervals with and without liposoluble Q₁₀ coreconstituted into the lipid phase. A steady (photostationary) state was approached slowly and bands were found to increase or decrease reversibly on illumination and relaxation. Tentative assignments were made for some bands, based on previous FTIR measurements. The long time scale of these processes was tentatively explained in terms of interprotein reactions of RC molecules.



INTRODUCTION

FTIR spectroscopy is well suited to investigate photoexcitation of bacterial reaction centers (RCs). RCs have been investigated either in chromatophores¹ of the respective bacteria or in purified and solubilized form, mostly as a rehydrated thin film between two CaF₂ windows.^{2–8} Marker bands for quinol formation were identified, obtained from the quinone/quinol pool present within chromatophores or added to solubilized RCs. Steady-state, light-minus-dark difference absorbance spectra under continuous illumination^{5,9–12} and time-resolved spectra^{1,3,4,7,13} have been measured. In the majority of these studies, the RCs have been observed in the presence of an electron donor to reduce the oxidized primary electron donor, P870⁺.^{1,7–9,12,14} Other redox active compounds have also been added as redox mediators.^{1,7,9,12,14}

We use a different strategy using surface-enhanced IR absorption spectroscopy (SEIRAS) according to which FTIR spectra are measured in the ATR configuration, with a thin structured gold film on the ATR crystal to achieve enhancement of the IR signal. Purified RCs can be immobilized as a monolayer on the surface of the gold film via his-tag, a technology also used for the measurement of photocurrents.^{15–18} In previous SEIRAS studies of cytochrome *c* oxidase (CcO), we had extended this strategy by in situ dialysis of the protein monolayer in the presence of lipid micelles. The

protein is thus reconstituted in a lipid bilayer to form a protein-tethered bilayer lipid membrane (ptBLM) (Figure 1).^{19,20} As a benefit of this structure, liposoluble Q₁₀ can be coreconstituted into the lipid phase, while the protein is preserved in a fully functional form.

MATERIALS AND METHODS

Solvents and Chemicals. Deionized water was used from a Sartorius-Stedim system (Goettingen, Germany) with a resistivity of 18 MΩ cm. Argon 4.8 was obtained from Linde Gas GmbH (Stadl-Paura, Austria). 3-Mercaptopropyltrimethoxysilane (MPTES, 95%) was purchased from ABCR GmbH (Karlsruhe, Germany). Gold granules (99.99%) for evaporation were obtained from Mateck GmbH (Juelich, Germany). Biobeads (20–50 mesh) were purchased from Bio-Rad Laboratories GmbH (Vienna, Austria). 1,2-Diphytanoyl-*sn*-glycero-3-phosphocholine (DiPhyPC, >99%) was provided by Avanti Polar Lipids (Alabaster, AL). Dithiobis (nitroacetate acid butylamidyl propionate) (DTNTA, ≥95.0%) was obtained from Dojindo Laboratories (Kumamoto, Japan). Hydroxylamine hydrochloride (NH₂OH.HCl, 99%), gold(III) chloride

Received: June 7, 2013

Revised: July 11, 2013

Published: July 18, 2013

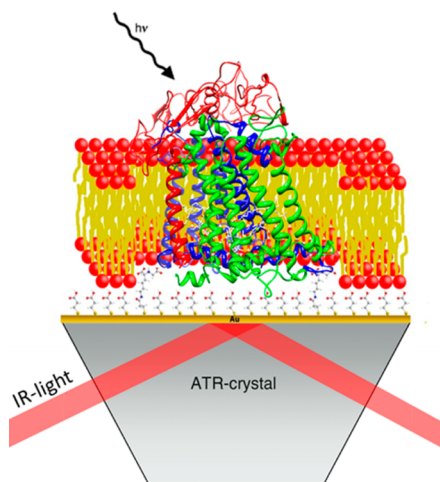


Figure 1. Setup of RCs immobilized on NTA-functionalized gold surface and reconstituted in the ptBLM. RCs are immobilized with the special pair oriented toward the surface of a silicon ATR crystal, covered with a two-layer gold film.

hydrate ($\text{HAuCl}_4 \cdot x\text{H}_2\text{O}$, 99.999%), dimethyl sulfoxide (DMSO, puriss., dried over molecular sieve), 3,3'-dithiodipropionic acid (DTP, 99%), dodecyl- β -D-maltoside (DDM, $\geq 98\%$), nickel(II) chloride (NiCl_2 , 98%), D-(+)-glucose ($\text{C}_6\text{H}_{12}\text{O}_6$, $\geq 99.5\%$), glucose oxidase (GOx), and catalase, as well as Coenzyme Q_{10} (Q-2, diisoprenyl-ubiquinone) were purchased from Sigma-Aldrich (Steinheim, Germany). All chemicals were used as purchased.

Preparation of the Two-Layer Gold Surface on the ATR Crystal. Preparation was done as previously described by Nowak et al.²¹ A polished silicon attenuated total reflection (ATR) crystal was immersed in a 10% ethanolic solution of MPTES for 60 min to anchor the gold layer. After rinsing with ethanol, the crystal was dried under a stream of argon and annealed at 100 °C for 60 min. The crystal was allowed to cool to room temperature, then immersed in water for 10 min, and dried under a stream of argon. A 25 nm gold film was then deposited onto the ATR crystal by electrochemical evaporation (HHV Edwards Auto 306, Crawley, U.K.). Gold nanoparticles were grown on the gold film by immersing the crystal in 50 mL of an aqueous solution of hydroxylamine hydrochloride (0.4 mM), to which 500 μL of an aqueous solution of gold(III) chloride hydrate (0.3 mM) was added five times at 2 min intervals. After that, the Au surface clearly showed protruding structures ranging in diameter from 43 to 60 nm (average 57 nm) with an aspect ratio of around 12. Finally, the crystal was rinsed with water and dried under a stream of argon.

Immobilization of the Protein. Wild-type *Rhodobacter sphaeroides* RCs with a genetically engineered 7-his-tag at the C-terminus of the M-subunit were expressed from a strain kindly provided by S.G. Boxer.²² RCs were purified according to a modification of the original method.²³ The immobilization of RC on either the template stripped gold (TSG) surface (see Supporting Information, SI) or the ATR crystal was performed according to a method described by Nowak et al.²⁴ and references therein. TSG was used for Surface Plasmon Resonance (SPR) Spectroscopy and Electrochemical Impedance Spectroscopy (EIS) (see SI). Briefly, the gold surface was immersed in a solution of 2.5 mM DTNTA and 7.5 mM DTP in dry DMSO for 20 h. After rinsing with ethanol and purified water, the surface was immersed in 40 mM NiCl_2 in acetate

buffer (50 mM, pH 5.5) for 30 min, followed by thorough rinsing with purified water to remove excess NiCl_2 . The surface was dried under a stream of argon prior to assembly in the measuring cell and rehydrated with DDM-DPK buffer (0.05 M K_2HPO_4 , 0.1 M KCl, pH 8, 0.1% DDM) before starting the SEIRA measurements. SEIRA spectra (Figure 2) were taken

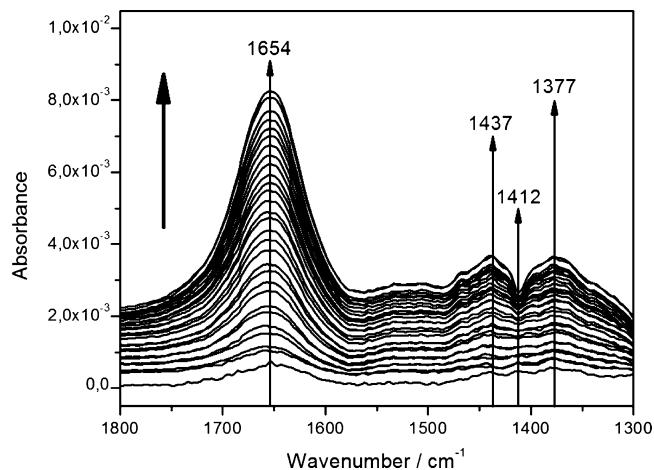


Figure 2. SEIRA spectra of RCs in the course of their immobilization on the gold film as a function of adsorption time. Total adsorption time was 4 h, intervals between spectra were 10 min. The spectrum of the functionalized gold surface was used as the reference.

while RCs dissolved in DDM-DPK were adsorbed to the NTA-functionalized gold surface at a final concentration of 100 nM. After 4 h time of adsorption carried out at 28 °C, the cell was rinsed with DDM-DPK to remove unspecifically adsorbed and bulk protein. Thereafter, DDM-DPK was replaced by a DiPhyPC/DDM-DPK solution (40 μM DiPhyPC in DDM-DPK). In the case of additional ubiquinone, Q_{10} was solubilized together with DiPhyPC (6 μM Q_{10} in DiPhyPC/DDM-DPK). In both cases, DDM was removed by adding Biobeads to the lipid-detergent solution.

ATR-SEIRA-Spectroscopy. The electrochemical cell was mounted on top of a trapezoid single reflection silicon ATR crystal. The IR beam of the FTIR spectrometer (VERTEX 70v, from Bruker, Ettlingen, Germany) was coupled into the crystal at an angle of incidence $\Theta = 60^\circ$ by using the custom-made setup described previously.²¹ All spectra were measured with parallel polarized light. Because the ATR element surface is coated with an electrical conductor, perpendicularly polarized light is unable to effectively penetrate the conducting layer. The total reflected IR beam intensity was measured with a liquid nitrogen-cooled photovoltaic mercury cadmium telluride (MCT) detector. IR measurements were done under aerobic conditions at 28 °C. The sample unit was purged with dry, carbon dioxide-free air. FTIR spectra were recorded at 4 cm^{-1} resolution using Blackham-Harris 3-term apodization and a zero filling factor of 2. The interferograms were measured in double-sided mode and transformed into spectra using the Power phase correction mode. Spectra were analyzed using the software package OPUS 7 and OriginLab's Origin software.

Illumination was performed with white light from a Fiber-Lite DC950 illuminator (150 W, quartz halogen lamp) provided with an optical fiber obtained from Dolan-Jenner (Boxborough, MA) with a light intensity of 0.2 W/cm^{-2} (at a wavelength of 800 nm).

RESULTS AND DISCUSSION

Formation of the ptBLM. Immobilization of the RCs and subsequent formation of the ptBLM followed by Surface Plasmon Resonance (SPR) and Electrochemical Impedance Spectroscopy (EIS) is shown in Figures S1 and S2A,B, respectively of the SI. Optical thickness and electrical parameters are given in Table S1 of the SI correspond to the respective data found in the case of CcO, where the surface concentration was determined to be $\sim 6 \text{ pMol cm}^{-2}$, in agreement with the calculated value for a densely packed monolayer from the crystal structure of CcO from *R. sphaeroides*.^{19,24,25} We conclude that a monolayer of RCs of a similar packing density had been formed on the gold film, with only small voids left between single proteins to be filled with a lipid bilayer.

SEIRAS Measurements. SEIRA spectra were recorded as a function of time in the course of the binding of the RCs via his-tag attached to the P side of the protein (Figure 2).

Vibrational components of α -helices in the amide I region can be recognized at 1654 cm^{-1} , as well as two bands at 1437 and 1377 cm^{-1} . The negative band at 1412 cm^{-1} may be due to changes in the NTA structure/orientation during complex formation with the his-tag.²⁶ No amide II bands are seen in the spectra. This can be explained in terms of the theory of SEIRAS, predicting that dipoles oriented perpendicular to the surface are subject to a particularly high surface-enhancement effect, while dipoles pointing in other directions are not detected.²⁷ Moreover, the enhancement decreases with distance from the metal film. The RCs are arranged on the surface with the α -helices pointing in the z-direction, giving rise to the relatively high absorbance of the amide I band. The transition dipole moment for the amide II mode is roughly orthogonal to this, with negligible SEIRA enhancement and consequently much weaker absorbance.

Next, light-minus-dark difference spectra were recorded under continuous illumination of the RC reconstituted in the ptBLM, first without any additional Q_{10} . A total of 1000 scans were recorded and averaged for every spectrum. Surprisingly, a steady state was not obtained on the seconds time scale, as described by Breton,⁶ for example. Instead, absorbances of many bands increased over a much longer time scale. The first spectrum taken after 5 min illumination time, with no additional Q_{10} , is shown in Figure 3. Next, spectra were recorded at 5 min intervals, also without additional Q_{10} (Figure 4), and band areas of selective peaks were plotted as a function of time (Figure 5A). A steady state is approached after >20 min.

As seen in the spectra, a number of positive bands appear at 1234 , 1282 , 1360 , 1434 , 1507 , 1642 , and a negative band at 1685 cm^{-1} . Between the bands at 1360 and 1434 cm^{-1} , a small negative band is buried at 1389 cm^{-1} but is seen in the second derivative spectrum also shown in Figure 3B. Broad negative and positive bands appear at 3400 and 3629 cm^{-1} , respectively. The most prominent band at 1434 cm^{-1} is strongly indicative of a band assigned to QH_2 by FTIR,^{1,2,4,7} although associated bands at 1491 , 1470 , and 1375 cm^{-1} are not seen. An FTIR band at 1389 cm^{-1} is also attributed to QH_2 ,^{1,7} but the negative sign here is not consistent with the generation of QH_2 indicated by the positive band at 1434 cm^{-1} . The band at 1282 cm^{-1} is an FTIR marker band of P^+ .^{28–30} A band at approximately 1360 cm^{-1} has been assigned to the δCH_3 vibration of the methyl group at the 5-position of the ring in the semiquinone difference spectra, between Q_A^- and Q_A and Q_B^- and Q_B .^{11,31}

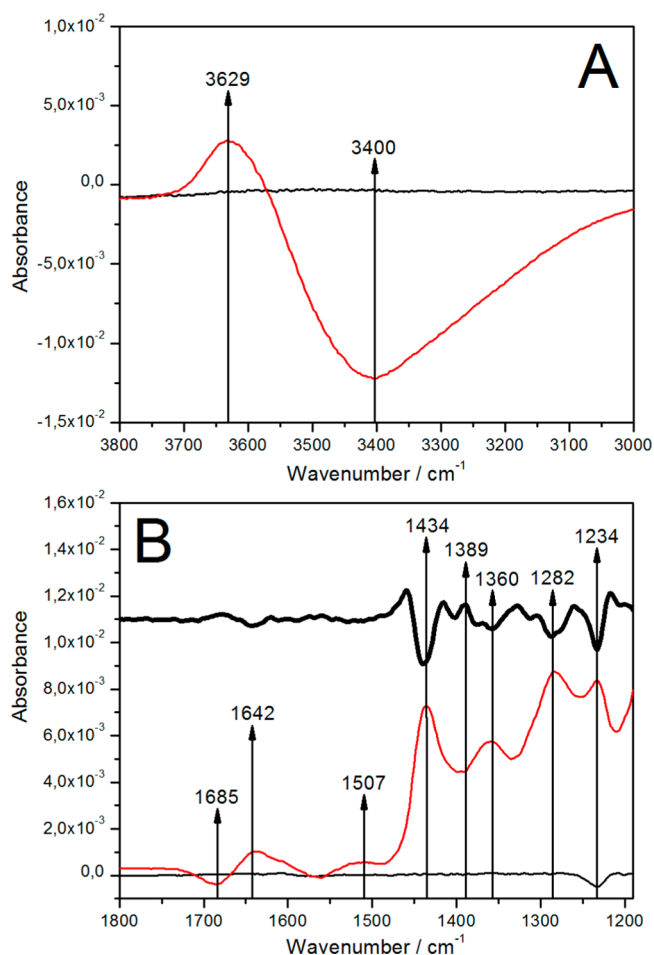


Figure 3. Light-minus-dark absorption spectra of RCs immobilized in the ptBLM after 5 min illumination time (red line), with the spectrum in the upper (A) and lower (B) wavenumber region. The reference spectrum in each is dark-minus-dark, which did not change as a function of time without illumination. The bold line in (B) represents the second-derivative spectrum showing a negative band appearing at 1389 cm^{-1} between the 1434 and 1360 cm^{-1} bands. The second derivative also shows that the band at 1642 cm^{-1} is an overlap of a variety of bands, which, however, cannot be resolved into single bands.

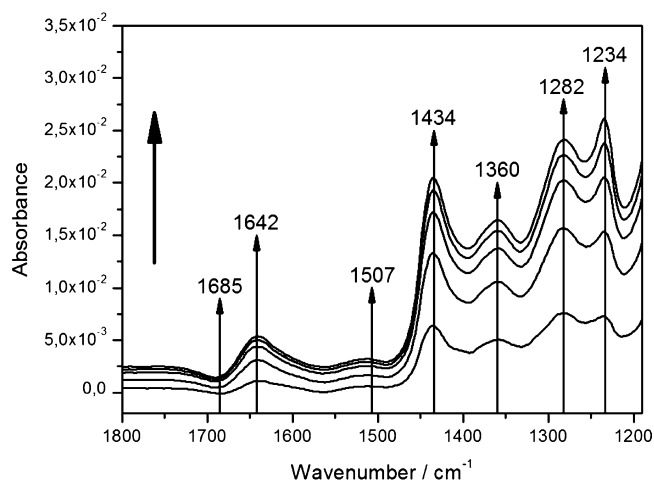


Figure 4. Time evolution of light-minus-dark absorption spectra of RCs immobilized in the ptBLM without added Q_{10} during the course of continuous illumination. Difference spectra were recorded every 5 min.

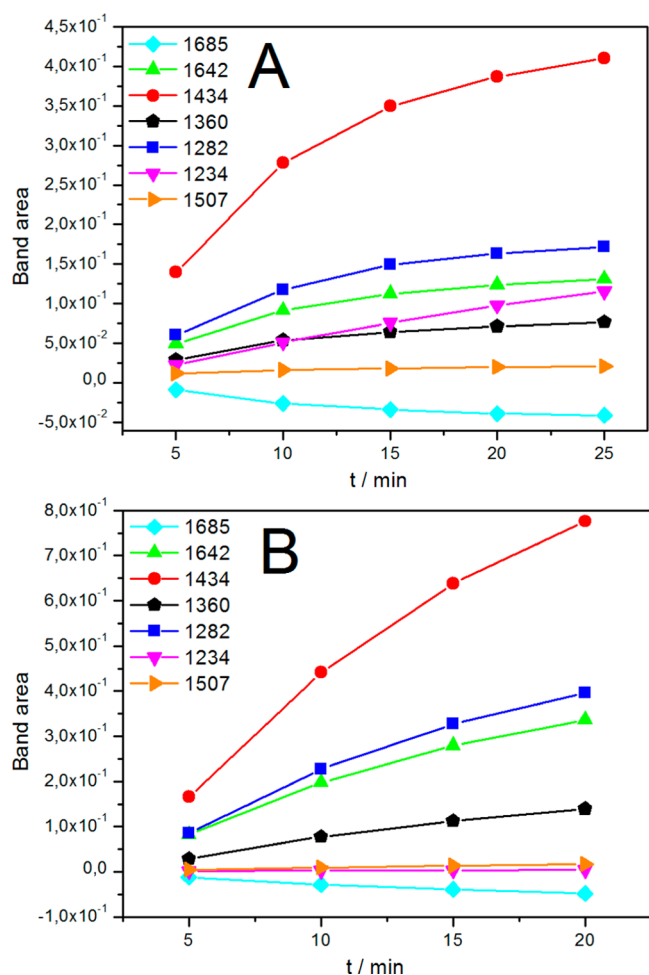


Figure 5. Band areas of absorbances of characteristic bands under continuous illumination of RCs in the ptBLM taken at different time intervals without (A) and with added Q_{10} (B).

FTIR bands indicating semiquinone were reported to occur at 1446 and 1479 cm^{-1} , which we do not see in our spectra.^{11,31} The band at 1642 cm^{-1} may be an overlap of several bands in the region of the amide I band of α -helices and H–O–H bending vibration of water, and the C=O stretching vibration of Q_B is also assigned in this region.^{4–6,29,32,33} Negative evolution of the band at 1685 cm^{-1} attributed to the C=O stretching vibration of the 9-keto group of $P^{4,30}$ is consistent with a decrease in the concentration of P.

Broad positive and negative bands in the region 3800–3000 cm^{-1} in FTIR were interpreted by Iwata et al.¹⁴ as water stretching vibrations associated with formation of either semiquinone, Q_A^- or Q_B^- . Given the orientation of the RC

in the ptBLM, with P facing the gold surface, oriented water(s) close to P/ P^+ are also a likely a source of these bands. It is noteworthy that the spectra exhibit a well-defined isosbestic point.

An assignment for the band at 1507 cm^{-1} could not be found in the literature. A band at 1234 cm^{-1} also could not be found in the literature dealing with RCs, but lies in the region of C–O stretching modes of carboxylic acids.³⁴ The latter, however, is a prominent recurrent band, which also remains after relaxation of all others (see below). It could not be correlated to any kind of alteration, for example addition of Q_{10} , time of illumination or relaxation, etc.

Tentative band assignments from previous FTIR measurements are collected in Table 1.

The origin of the bands discussed above was supported by spectra recorded with liposoluble Q_{10} coreconstituted into the lipid phase. The absorbance of the strong bands was shown to increase under illumination and to decrease during dark relaxation (Figures 6, 7, and 8). Absorbances also increased when Q_{10} was coreconstituted (Figures 5B and 6), showing that the evolution of these bands is affected by the quinone/quinol pool. In summary, in the approach to steady state under continuous illumination, we detected the evolution of QH_2 and P^+ occurring in the time scale of minutes, which is fully reversible after switching of the light. The long time scale of the reactions will be discussed further below.

CONCLUSIONS

Many of the bands found in our spectra can be correlated with bands reported in previous FTIR work (see Table 1). However, the overall appearance of the spectra is strikingly different from FTIR difference spectra found in the literature, which are usually composed of narrow peaks and troughs changing in the μs to s time scale.²⁹ Some of the unfamiliar features of our spectra can be explained by the theory of SEIRAS, notably the high sensitivity of vibrational components in close proximity to the surface, and the strong dependence on the orientation of the transition dipole moments, which must be oriented perpendicular to the surface.^{27,35} This means that the same component present in different orientations may be strongly represented or not at all. This largely accounts for the different sensitivities of bands associated with the same functional group, e.g., bands that represent QH_2 at 1434, 1491, 1470 cm^{-1} , of which only 1434 cm^{-1} is definitively seen here. This effect is enhanced by the preorientation of the RC molecules within the ptBLM. Furthermore, the extreme dominance of positive bands throughout the spectrum may indicate a strong effect of the large, internal dipole moment of the RC in the charge-separated state. The theory of SEIRAS, however, is not able to explain other features of our spectra, such as the substantial

Table 1. Possible Assignments of SEIRAS Bands for RCs Reconstituted in the ptBLM under Continuous Illumination

band (cm^{-1})		tentative assignment		
experimental	fwhm	literature	species	component
1282	77.5	1282 ^{28–30}	P^+	(complex)
1360	34.7	1355, ¹¹ 1365 ³²	Q_A	δCH_3
1434	25.7	1433 ^{1,2,4,7}	QH_2	
1643	66.7	1640, ^{5,29} 1641, ^{6,32,33} 1642 ⁴	quinone Q , Q_B	C=O
1685	35.2	1682, ³⁰ 1683 ⁴	9-keto group of P	C=O
3400	312.7	3485 ¹⁴	Q_B^-/Q_B or P^+	H_2O
3629	194.5	3632 ¹⁴	Q_B^-/Q_B or P^+	H_2O

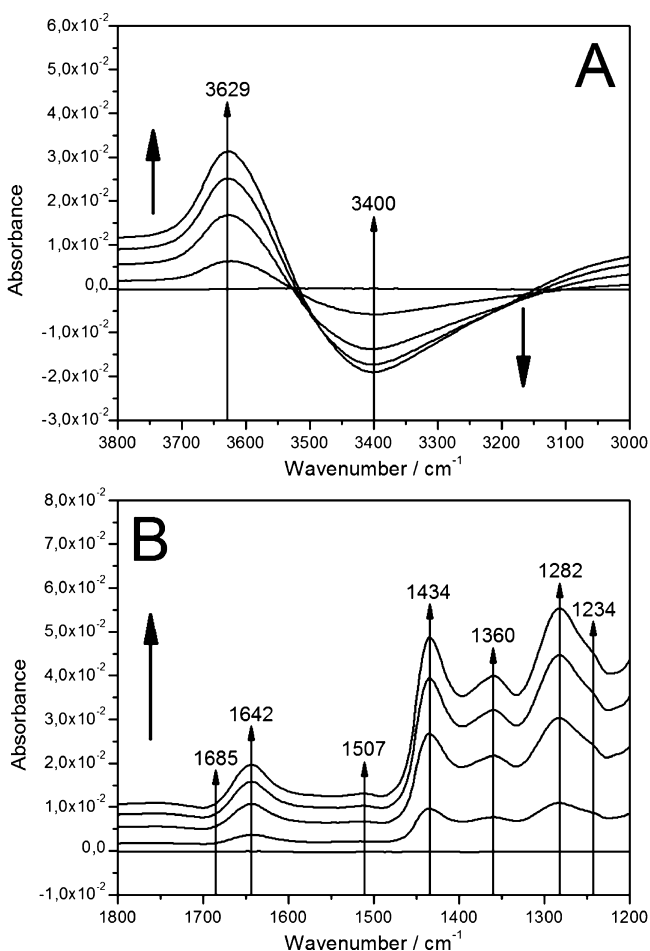


Figure 6. Light-minus-dark spectra of RCs in the ptBLM under continuous illumination with coreconstituted Q_{10} , with the spectrum in the dark as the reference, in the upper (A) and lower (B) wavenumber region. Difference spectra were recorded every 5 min.

enhancement in bandwidth, although this is also observed in other membrane proteins and we have speculated previously on possible origins.³⁶

The long time scale of the evolution of the SEIRA spectra, which we take to represent species such as P^+ and QH_2 , is unexpected. In FTIR, the light-driven electron transfers to form Q_A^- and Q_B^- (and even Q_B^{2-} or Q_BH_2) have been studied extensively in the μs to s time range. However, the release of QH_2 from its binding pocket and its replacement by a quinone molecule from the quinone pool have received attention only relatively recently.^{37–39} Multiple saturating flashes or continuous illumination of chromatophores from *R. sphaeroides* have revealed the slow accumulation of QH_2 , but in the presence of ascorbate and other redox mediators.¹ This investigation was later extended to look at intermediate RC states, using rapid scan FTIR spectroscopy of detergent micelles of RCs.⁷ Kinetic traces were analyzed in terms of a model taking into account the slow quinone exchange between RC micelles and pure detergent micelles, taking place in the time scale of seconds.^{7,40,41}

In all of these studies, however, multiple excitations were possible because of the presence of electron donors to restore P^+ back to P. These are absent in our experiments. The slow time scale of the formation of species such as QH_2 (and/or Q_BH_2) and P^+ (as indicated by probable assignments from

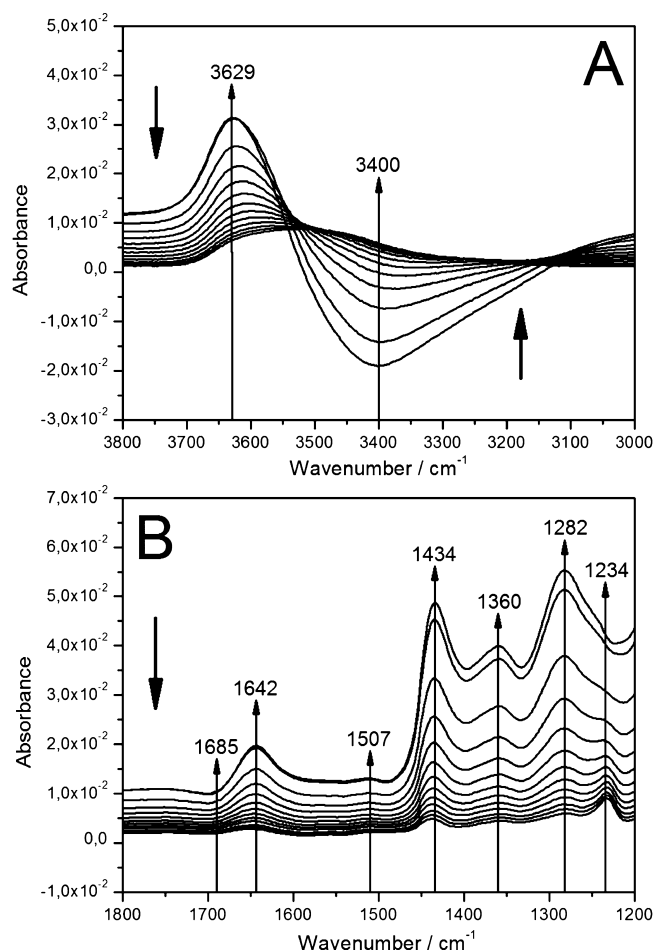


Figure 7. Relaxation of the bands of RC in the ptBLM with coreconstituted Q_{10} after termination of continuous illumination in the upper (A) and lower (B) wavenumber region. Total relaxation time is 1 h, difference spectra were recorded every 5 min.

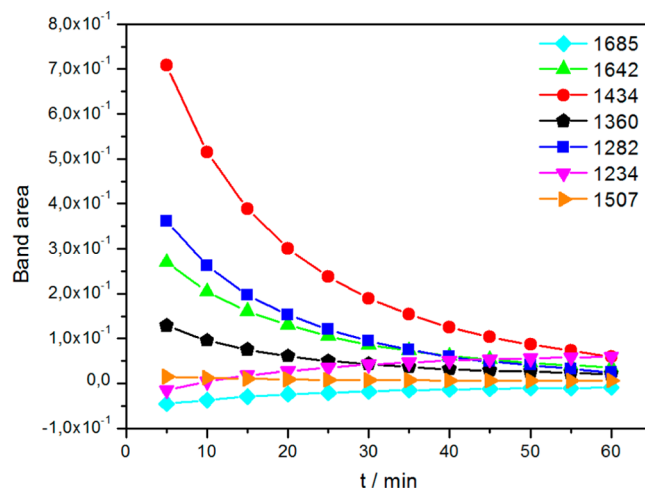


Figure 8. Kinetics of characteristic bands during relaxation. All band areas decrease during relaxation except for bands at 1234 and 1685 cm^{-1} , which increase.

FTIR marker bands), in the absence of an electron donor, suggests the following possible explanation. Due to the high density of RCs, interprotein quinone/semiquinone exchange may become possible, allowing release of quinol into the

membrane. Under normal circumstances the states $P^+Q_A^-$ and $P^+Q_B^-$ recombine in 0.1–1 s and these would represent the only detectable states, depending on light intensity. At the high protein densities used here, however, it may be possible for some cross reactivity to occur, i.e., $P^+Q_B^- + P^+Q_B^- \rightarrow P^+Q_B + P^+Q_B^{2-}$, followed by protonation of Q_B^{2-} and release as QH_2 into the membrane, with rebinding of Q_B from the quinone pool. The resulting states, P^+Q_B and QH_2 , can be expected to be quite long-lived and to accumulate slowly over time. The fact that all or most of the light-induced SEIRA bands exhibit similar kinetics is supportive of this model. During relaxation, restoration of the dark adapted state would mostly likely be associated with direct reduction of P^+ by QH_2 , yielding a short-lived semiquinone that would reduce another P^+ . However, reversal of the original disproportionation is also possible: $2P^+Q_B + QH_2 \rightarrow P^+Q_B^{2-} + P^+Q_B \rightarrow P^+Q_B^- + P^+Q_B^-$.

Another characteristic of the SEIRA spectra is the full width at half-maximum (fwhm) of the bands, which is significantly larger than that of the sharp bands found in the FTIR literature.²⁹ The fwhm is generally related to the freedom of movement of the structure associated with the particular component.^{42–44} In previous studies, the protein was investigated either in the presence of an electron donor, or even an entire cocktail of mediators. In a previous SEIRAS study of cytochrome *c* oxidase, we observed the narrowing of fwhm in the presence of mediators.^{24,36} The effect might be explained in terms of the internal dipole potential of the naturally activated charge-separated state being markedly different from that after equilibration between mediators and redox sites.

The positive and negative bands in the region 3800–3000 cm^{-1} should be due to highly ordered water molecules,¹⁴ which are known to have particularly strong transition dipole moments. Remarkable in this context is a clear isosbestic point for these bands indicating that only *two* species vary in concentration to contribute to the absorption. The near-constancy of the isosbestic point also indicates that temperature effects should be small in this region.

In summary, SEIRAS of RCs present within a ptBLM yields a number of strong bands at wavelengths that correlate them with FTIR marker bands of photoexcitation. Weaker signals may be buried underneath the strong bands, potentially contributing to the large, apparent fwhm of the major bands. The time-evolution of the SEIRA spectra is, however, unusually slow and not as observed in other experimental setups. The long time scale is consistent with the idea of an interprotein disproportionation reaction followed by QH_2/Q exchange, which is diffusional. Reversal of the disproportionation accounts for the almost complete reversibility of the reactions observed under the experimental conditions used here.

■ ASSOCIATED CONTENT

● Supporting Information

Additional Information about preparation of Template Stripped Gold (TSG), Surface Plasmon Resonance Spectroscopy (SPR) measurements, and Electrochemical Impedance Spectroscopy (EIS) used to monitor the immobilization of the protein and membrane formation. This material is available free of charge via the Internet at <http://pubs.acs.org>.

■ AUTHOR INFORMATION

Corresponding Author

*Phone: 0043 664 6207708, e-mail: Renate.Naumann@ait.ac.at.

Notes

The authors declare no competing financial interest.

■ ACKNOWLEDGMENTS

C.A.W. gratefully acknowledges support by NSF Grant MCB 08-18121.

■ REFERENCES

- (1) Mezzetti, A.; Leibl, W.; Breton, J.; Nabdryk, E. Photoreduction of the quinone pool in the bacterial photosynthetic membrane: identification of infrared marker bands for quinol formation. *FEBS Lett.* **2003**, *537*, 161–165.
- (2) Mezzetti, A.; Blanchet, L.; Juan, A.; Leibl, W.; Ruckebusch, C. Ubiquinol formation in isolated photosynthetic reaction centres monitored by time-resolved differential FTIR in combination with 2D correlation spectroscopy and multivariate curve resolution. *Anal. Bioanal. Chem.* **2010**, *399*, 1999–2014.
- (3) Hermes, S.; Stachnik, J. M.; Onidas, D.; Remy, A.; Hofmann, E.; Gerwert, K. Proton uptake in the reaction center mutant L210DN from *Rhodobacter sphaeroides* via protonated water molecules. *Biochemistry* **2006**, *45*, 13741–13749.
- (4) Brudler, R.; Gerwert, K. Step-Scan FTIR Spectroscopy Resolves the $Q(A)(-)Q(B) \rightarrow Q(A)Q(B)(-)$ Transition in *Rb-sphaeroides* R26 Reaction Centres. *Photosynth. Res.* **1998**, *55*, 261–266.
- (5) Breton, J.; Thibodeau, D. L.; Berthomieu, C.; Mantele, W.; Vermeglio, A.; Nabdryk, E. Probing the Primary Quinone Environment in Photosynthetic Bacterial Reaction Centers by Light-Induced FTIR Difference Spectroscopy. *FEBS Lett.* **1991**, *278*, 257–260.
- (6) Breton, J. Steady-State FTIR Spectra of the Photoreduction of $Q(A)$ and $Q(B)$ in *Rhodobacter sphaeroides* Reaction Centers Provide Evidence against the Presence of a Proposed Transient Electron Acceptor X between the Two Quinones. *Biochemistry* **2007**, *46*, 4459–4465.
- (7) Mezzetti, A.; Leibl, W. Investigation of Ubiquinol Formation in Isolated Photosynthetic Reaction Centers by Rapid-Scan Fourier Transform IR Spectroscopy. *Eur. Biophys. J.* **2005**, *34*, 921–936.
- (8) Brudler, R.; Degroot, H. J. M.; Vanliemt, W. B. S.; Gast, P.; Hoff, A. J.; Lugtenburg, J.; Gerwert, K. Ftir Spectroscopy Shows Weak Symmetrical Hydrogen-Bonding of the $Q(B)$ Carbonyl Groups in *Rhodobacter-Sphaeroides* R26 Reaction Centers. *FEBS Lett.* **1995**, *370*, 88–92.
- (9) Breton, J.; Berthomieu, C.; Thibodeau, D. L.; Nabdryk, E. Probing the Secondary Quinone (QB) Environment in Photosynthetic Bacterial Reaction Centers by Light-Induced FTIR Difference Spectroscopy. *FEBS Lett.* **1991**, *288*, 109–113.
- (10) Breton, J.; Burie, J. R.; Boullais, C.; Berger, G.; Nabdryk, E. Binding Sites of Quinones in Photosynthetic Bacterial Reaction Centers Investigated by Light-Induced FTIR Difference Spectroscopy: Binding of Chainless Symmetrical Quinones to the QA Site of *Rhodobacter sphaeroides*. *Biochemistry* **1994**, *33*, 12405–12415.
- (11) Breton, J.; Boullais, C.; Burie, J. R.; Nabdryk, E.; Mioskowski, C. Binding-Sites of Quinones in Photosynthetic Bacterial Reaction Centers Investigated by Light-Induced Ftir Difference Spectroscopy—Assignment of the Interactions of Each Carbonyl of $Q(a)$ in *Rhodobacter sphaeroides* Using Site-Specific C-13-Labeled Ubiquinone. *Biochemistry* **1994**, *33*, 14378–14386.
- (12) Breton, J.; Burie, J. R.; Berthomieu, C.; Berger, G.; Nabdryk, E. The Binding-Sites of Quinones in Photosynthetic Bacterial Reaction Centers Investigated by Light-Induced Ftir Difference Spectroscopy—Assignment of the $Q(a)$ Vibrations in *Rhodobacter sphaeroides* Using O-18-Labeled or C-13-Labeled Ubiquinone and Vitamin-K-1. *Biochemistry* **1994**, *33*, 4953–4965.

- (13) Mezzetti, A.; Blanchet, L.; de Juan, A.; Leibl, W.; Ruckebusch, C. Ubiquinol Formation in Isolated Photosynthetic Reaction Centres Monitored by Time-Resolved Differential FTIR in Combination with 2D Correlation Spectroscopy and Multivariate Curve Resolution. *Anal. Bioanal. Chem.* **2011**, *399*, 1999–2014.
- (14) Iwata, T.; Paddock, M. L.; Okamura, M. Y.; Kandori, H. Identification of FTIR Bands Due to Internal Water Molecules around the Quinone Binding Sites in the Reaction Center from *Rhodobacter sphaeroides*. *Biochemistry* **2009**, *48*, 1220–1229.
- (15) Trammell, S. A.; Wang, L.; Zullo, J. M.; Shashidhar, R.; Lebedev, N. Orientated Binding of Photosynthetic Reaction Centers on Gold Using Ni-NTA Self-Assembled Monolayers. *Biosens. Bioelectron.* **2004**, *19*, 1649–1655.
- (16) Trammell, S. A.; Griva, I.; Spano, A.; Tsoi, S.; Tender, L. M.; Schnur, J.; Lebedev, N. Effects of Distance and Driving Force on Photoinduced Electron Transfer between Photosynthetic Reaction Centers and Gold Electrodes. *J. Phys. Chem. C* **2007**, *111*, 17122–17130.
- (17) Lebedev, N.; Trammell, S. A.; Spano, A.; Lukashev, E.; Griva, I.; Schnur, J. Conductive Wiring of Immobilized Photosynthetic Reaction Center to Electrode by Cytochrome *c*. *J. Am. Chem. Soc.* **2006**, *128*, 12044–12045.
- (18) Lebedev, N.; Trammell, S. A.; Tsoi, S.; Spano, A.; Kim, J. H.; Xu, J.; Twigg, M. E.; Schnur, J. M. Increasing Efficiency of Photoelectronic Conversion by Encapsulation of Photosynthetic Reaction Center Proteins in Arrayed Carbon Nanotube Electrode. *Langmuir* **2008**, *24*, 8871–8876.
- (19) Friedrich, M. G.; Robertson, J. W. F.; Walz, D.; Knoll, W.; Naumann, R. L. C. Electronic Wiring of a Multi-Redox Site Membrane Protein in a Biomimetic Surface Architecture. *Biophys. J.* **2008**, *94*, 3698–3705.
- (20) Giess, F.; Friedrich, M. G.; Heberle, J.; Naumann, R. L.; Knoll, W. The Protein-Tethered Lipid Bilayer: A Novel Mimic of the Biological Membrane. *Biophys. J.* **2004**, *87*, 3213–3220.
- (21) Nowak, C.; Luening, C.; Knoll, W.; Naumann, R. L. C. A Two-Layer Gold Surface with Improved Surface Enhancement for Spectro-Electrochemistry Using Surface-Enhanced Infrared Absorption Spectroscopy. *Appl. Spectrosc.* **2009**, *63*, 1068–1074.
- (22) Goldsmith, J. O.; Boxer, S. G. Rapid Isolation of Bacterial Photosynthetic Reaction Centers with an Engineered Poly-Histidine Tag. *Biochim. Biophys. Acta, Bioenerg.* **1996**, *1276*, 171–175.
- (23) Kirmaier, C.; Laible, P. D.; Czarnecki, K.; Hata, A. N.; Hanson, D. K.; Bocian, D. F.; Holten, D. Comparison of M-Side Electron Transfer in *Rb. sphaeroides* and *Rb. capsulatus* Reaction Centers. *J. Phys. Chem. B* **2002**, *106*, 1799–1808.
- (24) Nowak, C.; Schach, D.; Gebert, J.; Grosserueschkamp, M.; Gennis, R. B.; Ferguson-Miller, S.; Knoll, W.; Walz, D.; Naumann, R. L. C. Oriented Immobilization and Electron Transfer to the Cytochrome *c* Oxidase. *J. Solid State Electrochem.* **2011**, *15*, 105–114.
- (25) Schach, D.; Nowak, C.; Gennis, R. B.; Ferguson-Miller, S.; Knoll, W.; Walz, D.; Naumann, R. L. C. Modeling Direct Electron Transfer to a Multi-Redox Center Protein Cytochrome *c* Oxidase. *J. Electroanal. Chem.* **2010**, *649*, 268–276.
- (26) Ataka, K.; Giess, F.; Knoll, W.; Naumann, R.; Haber-Pohlmeier, S.; Richter, B.; Heberle, J. Oriented Attachment and Membrane Reconstitution of His-Tagged Cytochrome *c* Oxidase to a Gold Electrode: In Situ Monitoring by Surface-Enhanced Infrared Absorption Spectroscopy. *J. Am. Chem. Soc.* **2004**, *126*, 16199–16206.
- (27) Osawa, M. Surface-Enhanced Infrared Absorption. *Top. Appl. Phys.* **2001**, *81*, 163–187.
- (28) Mäntele, W.; Nabedryk, E.; Tavitian, B. A.; Kreutz, W.; Breton, J. Light-Induced Fourier Transform Infrared (FTIR) Spectroscopic Investigations of the Primary Donor Oxidation in Bacterial Photosynthesis. *FEBS Lett.* **1985**, *187*, 227–232.
- (29) Remy, A.; Gerwert, K. Coupling of Light-Induced Electron Transfer to Proton Uptake in Photosynthesis. *Nat. Struct. Biol.* **2003**, *10*, 637–644.
- (30) Leonhard, M.; Mäntele, W. Fourier-Transform Infrared-Spectroscopy and Electrochemistry of the Primary Electron-Donor in *Rhodobacter sphaeroides* and *Rhodospseudomonas viridis* Reaction Centers—Vibrational-Modes of the Pigments In Situ and Evidence for Protein and Water Modes Affected by P+ Formation. *Biochemistry* **1993**, *32*, 4532–4538.
- (31) Breton, J.; Boullais, C.; Berger, G.; Mioskowski, C.; Nabedryk, E. Binding Sites of Quinones in Photosynthetic Bacterial Reaction Centers Investigated by Light-Induced FTIR Difference Spectroscopy: Symmetry of the Carbonyl Interactions and Close Equivalence of the QB Vibrations in *Rhodobacter sphaeroides* and *Rhodospseudomonas viridis* Probed by Isotope Labeling. *Biochemistry* **1995**, *34*, 11606–11616.
- (32) Nabedryk, E.; Breton, J. Coupling of Electron Transfer to Proton Uptake at the QB Site of the Bacterial Reaction Center: A Perspective from FTIR Difference Spectroscopy. *Biochim. Biophys. Acta, Bioenerg.* **2008**, *1777*, 1229–1248.
- (33) Breton, J.; Nabedryk, E. Protein-Quinone Interactions in the Bacterial Photosynthetic Reaction Center: Light-Induced FTIR Difference Spectroscopy of the Quinone Vibrations. *Biochim. Biophys. Acta, Bioenerg.* **1996**, *1275*, 84–90.
- (34) Stuart, B. *Biological Applications of Infrared Spectroscopy*; John Wiley & Sons, Ltd: New York, 1997.
- (35) Jiang, X.; Zaitseva, E.; Schmidt, M.; Siebert, F.; Engelhard, M.; Schlesinger, R.; Ataka, K.; Vogel, R.; Heberle, J. Resolving Voltage-Dependent Structural Changes of a Membrane Photoreceptor by Surface-Enhanced IR Difference Spectroscopy. *Proc. Natl. Acad. Sci. U. S. A.* **2008**, *105*, 12113–12117.
- (36) Nowak, C.; Santonicola, M. G.; Schach, D.; Zhu, J.; Gennis, R. B.; Ferguson-Miller, S.; Baurecht, D.; Walz, D.; Knoll, W.; Naumann, R. L. C. Conformational Transitions and Molecular Hysteresis of Cytochrome *c* Oxidase: Varying the Redox State by Electronic Wiring. *Soft Matter* **2010**, *6*, 5523–5532.
- (37) Nabedryk, E.; Breton, J.; Okamura, M. Y.; Paddock, M. L. Proton Uptake by Carboxylic Acid Groups upon Photoreduction of the Secondary Quinone (Q(B)) in Bacterial Reaction Centers from *Rhodobacter sphaeroides*: FTIR Studies on the Effects of Replacing Glu H173. *Biochemistry* **1998**, *37*, 14457–14462.
- (38) Graige, M. S.; Paddock, M. L.; Bruce, J. M.; Feher, G.; Okamura, M. Y. Mechanism of Proton-Coupled Electron Transfer for Quinone (Q(B)) Reduction in Reaction Centers of *Rb-sphaeroides*. *J. Am. Chem. Soc.* **1996**, *118*, 9005–9016.
- (39) McPherson, P. H.; Schonfeld, M.; Paddock, M. L.; Okamura, M. Y.; Feher, G. Protonation and Free Energy Changes Associated with Formation of QBH2 in Native and Glu-L212 → Gln Mutant Reaction Centers from *Rhodobacter sphaeroides*. *Biochemistry* **1994**, *33*, 1181–1193.
- (40) Shinkarev, V. P.; Wraight, C. A. The Interaction of Quinone and Detergent with Reaction Centers of Purple Bacteria 0.1. Slow Quinone Exchange between Reaction Center Micelles and Pure Detergent Micelles. *Biophys. J.* **1997**, *72*, 2304–2319.
- (41) Blanchet, L.; Mezzetti, A.; Ruckebusch, C.; Huvenne, J. P.; de Juan, A. Multivariate Curve Resolution of Rapid-Scan FTIR Difference Spectra of Quinone Photoreduction in Bacterial Photosynthetic Membranes. *Anal. Bioanal. Chem.* **2007**, *387*, 1863–1873.
- (42) Mantsch, H. H.; McElhaney, R. N. Phospholipid Phase-Transitions in Model and Biological-Membranes as Studied by Infrared-Spectroscopy. *Chem. Phys. Lipids* **1991**, *57*, 213–226.
- (43) Arrondo, J. L. R.; Castresana, J.; Valpuesta, J. M.; Goni, F. M. Structure and Thermal-Denaturation of Crystalline and Noncrystalline Cytochrome-Oxidase as Studied by Infrared-Spectroscopy. *Biochemistry* **1994**, *33*, 11650–11655.
- (44) Casal, H. L.; Cameron, D. G.; Smith, I. C. P.; Mantsch, H. H. *Acholeplasma laidlawii* Membranes: A Fourier Transform Infrared Study of the Influence of Protein on Lipid Organization and Dynamics. *Biochemistry* **1980**, *19*, 444–451.